MULTI-PHOTO COMBINED ADJUSTMENT WITH AIRBORNE SAR IMAGES BASED ON F.LEBERL ORTHO-RECTIFICATION MODEL

X.J. Yue [a, b,*], G.M. Huang [a, b], Y. Zhang [c], Z.Zhao [b], L.Pang [b]

[a] School of Geodesy and Geomatics, Wuhan University, 129 Luoyu Road, Wuhan-(xijuanyue, huang.guoman) @163.com
[b] Chinese Academy of Survey and Mapping, 16 Beitaiping Road, Beijing-zhengzhao@casm.ac.cn
[c] National Earthquake Infrastructure Service, 63 Fuxing Road, Beijing-yzhang@gps.gov.cn

KEY WORDS: Airborne SAR, F.Leberl Model, Ortho-rectification, GCPs, Pass Points, Multi-photo Combined Adjustment

ABSTRACT:

This paper introduces an ortho-rectification method of airborne SAR images which is multi-photo combined adjustment method based on F.Leberl imaging model. Multi-photo combined adjustment model of airborne SAR images is built. Multi-photo combined adjustment conditions are given in this paper. This method is applicable to multi-temporal, multi-side-looking-orientation, multi-flight-height, multi-resolution SAR Images. Two adjustment experiments have been done with one-meter resolution airborne SAR images in Chengdu study site. In the two experiments, the GCPs and the Pass Points are distributed rationally in each image. The two experimental results show that the coordinate accuracy of Pass Points is feasible for 1:10 000 scale ortho-image making and topographic map updating. There are four images in the first experiment, and nine GCPs and ten Pass Points are used. There are eleven images in the second experiment, and nine GCPs and thirty Pass Points are used. The second experimental result is better than the first one. Because the Pass Points are twice overlap in the first experiment and the most Pass Points are more than twice overlap in the second one.

1. INTRODUCTIONS

There are many perennially cloudy, misty and rainy regions in China. Therefore optical images are acquired very difficultly in these areas. A new approach to obtain mapping data in these areas is given by Synthetic Aperture Radar (SAR) which is all-weather and all-time. In these years, State Bureau of Surveying and Mapping of China have done airborne SAR mapping experiments in Zhengzhou Henan province and Zigong, Chengdu Sichuan province, in order to solve geometry rectification of high resolution airborne SAR images(Huang G.M. et al, 2008). In digital photogrammetry age, the formats of imaging models have not been difficulties of solution. F. Leberl imaging model accords with SAR imaging mechanism, and are independent from the attitude parameters of the sensor, only relates to the position, flight velocity and orientation of the sensor. So there are a few rectification parameters in F. Leberl imaging model(Zhu C.Y. et al, 2003). It is easy and effective to geometry rectification and object positioning of SAR images which are range projection.

This paper introduces a geometry rectification method of airborne SAR images which is multi-photo combined adjustment method based on F. Leberl imaging model. Multi-photo combined adjustment model of airborne SAR images is built. Multi-photo combined adjustment conditions are given. The influence of pass point accuracy due to the number and distribution of Ground Control Points (GCPs) and pass points is analyzed in this paper.

2. MODEL AND SOLUTION

2.1 Multi-photo Combined Adjustment Model Based on F. Leberl Imaging Equations

F. Leberl imaging equations are mathematical equations that determine the position of image points in image space coordinate system based on geometric characters of SAR imaging. There are two geometric conditions used in SAR imaging. One is range condition in across-track, the other is Doppler condition in along-track(Franz Leberl, 1978; G. Domik, Franz Leberl,1988).

2.1.1 Range Condition: Function (1) is about it in slant range image.

$$(X - X_s)^2 + (Y - Y_s)^2 + (Z - Z_s)^2 = (D_s + m_y \cdot y)^2 \quad (1)$$

where (X, Y, Z) = ground coordinate

(X_s, Y_s, Z_s) = position of radar antenna in SAR imaging

D_s = scanning delay or initial slant range

m_y = resolution of SAR image in across-track

y = image coordinate of SAR image in across-track

2.1.2 Doppler Condition: Airborne SAR image covers a little area, so the effect of earth's rotation can be ignored. That is vertical between radar beam and aircraft flight track, and Doppler frequency is zero(Shu N., 2003; Wang D.H., Liu J., Zhang L., 2005). Function (2) is about it.

$$u_x(X - X_s) + u_y(Y - Y_s) + u_z(Z - Z_s) = 0 \quad (2)$$

where (u_x, u_y, u_z) = velocity vector of aircraft flight

There is linear relation between image coordinate and time, and (u_x, u_y, u_z) is the function of time(Xiao G.C. Zhu C.Y., 2001; Fan H.D., 2007). As follows:

$$\begin{aligned} T &= m_x \cdot x \\ X_s &= a_0 + a_1 T + a_2 T^2 + a_3 T^3 \\ Y_s &= b_0 + b_1 T + b_2 T^2 + b_3 T^3 \\ Z_s &= c_0 + c_1 T + c_2 T^2 + c_3 T^3 \\ u_x &= a_1 + 2a_2 T + 3a_3 T^2 \\ u_y &= b_1 + 2b_2 T + 3b_3 T^2 \\ u_z &= c_1 + 2c_2 T + 3c_3 T^2 \end{aligned} \quad (3)$$

where

T = time

m_x = resolution of SAR image in along-track

x = image coordinate of SAR image in along-track

Function (3) is carried in Function (1) and Function (2), and F. Leberl imaging equations are obtained. Function (4) is about it.

$$\begin{aligned} f &= (D_s + m_y \cdot y) - [(X - (a_0 + a_1 T + a_2 T^2 + a_3 T^3))^2 \\ &\quad + (Y - (b_0 + b_1 T + b_2 T^2 + b_3 T^3))^2 \\ &\quad + (Z - (c_0 + c_1 T + c_2 T^2 + c_3 T^3))^2]^{\frac{1}{2}} \\ g &= (a_1 + 2a_2 T + 3a_3 T^2) \cdot (X - (a_0 + a_1 T + a_2 T^2 + a_3 T^3)) \\ &\quad + (b_1 + 2b_2 T + 3b_3 T^2) \cdot (Y - (b_0 + b_1 T + b_2 T^2 + b_3 T^3)) \\ &\quad + (c_1 + 2c_2 T + 3c_3 T^2) \cdot (Z - (c_0 + c_1 T + c_2 T^2 + c_3 T^3)) \end{aligned} \quad (4)$$

Function (5) is differential and linearized equation about Function (4). It is error equation of multi-photo combined adjustment model.

$$\begin{bmatrix} Vf_1 \\ \vdots \\ Vf_n \\ Vg_1 \\ \vdots \\ Vg_n \end{bmatrix} = \begin{bmatrix} \frac{\partial f_1}{\partial a_0} & \cdots & \frac{\partial f_1}{\partial a_3} & \frac{\partial f_1}{\partial b_0} & \cdots & \frac{\partial f_1}{\partial b_3} & \frac{\partial f_1}{\partial c_0} & \cdots & \frac{\partial f_1}{\partial c_3} & \frac{\partial f_1}{\partial X_1} & \frac{\partial f_1}{\partial Y_1} & \cdots & \frac{\partial f_1}{\partial X_k} & \frac{\partial f_1}{\partial Y_k} \\ \vdots & \cdots & \vdots & \vdots & \cdots & \vdots & \vdots & \cdots & \vdots & \vdots & \vdots & \cdots & \vdots & \vdots \\ \frac{\partial f_n}{\partial a_0} & \cdots & \frac{\partial f_n}{\partial a_3} & \frac{\partial f_n}{\partial b_0} & \cdots & \frac{\partial f_n}{\partial b_3} & \frac{\partial f_n}{\partial c_0} & \cdots & \frac{\partial f_n}{\partial c_3} & \frac{\partial f_n}{\partial X_1} & \frac{\partial f_n}{\partial Y_1} & \cdots & \frac{\partial f_n}{\partial X_k} & \frac{\partial f_n}{\partial Y_k} \\ \frac{\partial g_1}{\partial a_0} & \cdots & \frac{\partial g_1}{\partial a_3} & \frac{\partial g_1}{\partial b_0} & \cdots & \frac{\partial g_1}{\partial b_3} & \frac{\partial g_1}{\partial c_0} & \cdots & \frac{\partial g_1}{\partial c_3} & \frac{\partial g_1}{\partial X_1} & \frac{\partial g_1}{\partial Y_1} & \cdots & \frac{\partial g_1}{\partial X_k} & \frac{\partial g_1}{\partial Y_k} \\ \vdots & \cdots & \vdots & \vdots & \cdots & \vdots & \vdots & \cdots & \vdots & \vdots & \vdots & \cdots & \vdots & \vdots \\ \frac{\partial g_n}{\partial a_0} & \cdots & \frac{\partial g_n}{\partial a_3} & \frac{\partial g_n}{\partial b_0} & \cdots & \frac{\partial g_n}{\partial b_3} & \frac{\partial g_n}{\partial c_0} & \cdots & \frac{\partial g_n}{\partial c_3} & \frac{\partial g_n}{\partial X_1} & \frac{\partial g_n}{\partial Y_1} & \cdots & \frac{\partial g_n}{\partial X_k} & \frac{\partial g_n}{\partial Y_k} \end{bmatrix} \cdot \begin{bmatrix} da_0 \\ \vdots \\ da_3 \\ db_0 \\ \vdots \\ db_3 \\ dc_0 \\ \vdots \\ dc_3 \\ dX_1 \\ dY_1 \\ \vdots \\ dX_k \\ dY_k \end{bmatrix} - \begin{bmatrix} -f_1^0 \\ \vdots \\ -f_n^0 \\ -g_1^0 \\ \vdots \\ -g_n^0 \end{bmatrix} \quad (5)$$

where k = number of Pass Points

Because of low base-height ratio and low intersection angle of corresponding points, observation data in same side can be resulted in poor elevation accuracy. But multi-photo combined adjustment of observation data in different side can lead to geminate expense of data acquisition. The elevation value is obtained from 1:50,000 scale DEM, considered pass points as elevation points(Huang G.M. et al, 2008). There is no dX_i, dY_i about GCP.

2.2 Conditions of Multi-photo Combined Adjustment Model

nP photos are given, the number of GCPs is $nGCP$, the number of Pass Points is nJM. The total number of GCPs participated in calculation is $nCalGCP$, and the total number of Pass Points participated in calculation is $nCalJM$.

$$nCalGCP \geq nGCP \quad (6)$$

$$nCalJM \geq nJM \quad (7)$$

$$n = 2 \times (nCalGCP + nCalJM) \quad (8)$$

$$t = 12 \times nP + 2 \times nJM \quad (9)$$

where nP = number of photos given

$nGCP$ = number of GCPs

nJM = number of Pass Points

$nCalGCP$ = total number of GCPs participated in calculation

$nCalJM$ = total number of Pass Points participated in calculation

n = number of condition equations

t = number of necessary observation

In order to satisfying adjustment condition of ortho-rectification coefficients' calculation, the total number of GCPs and Pass Points is more than 6 in each image. In order to satisfying multi-photo combined adjustment condition, n is bigger than t.

2.3 Solution Process

2.3.1 Initial Value Solution: Initial value is divided into two parts as follows. One is ground coordinates of pass point (X_0, Y_0, Z_0), the other is ortho-rectification coefficients of each image a_{0i}, b_{0i}.

(1)Initial value of ground coordinates of pass points

Selecting appropriate corresponding image points as tie points in overlap section of adjoining images. Simple or quadric polynomial transform models are built between image coordinates of corresponding image points, then transform coefficients are gotten from top to bottom, from left to right, based on the image of the top left corner, and then all image coordinates are unified as the same coordinates system of the image of the top left corner. According to horizontal coordinates of GCPs (X, Y) and corresponding image coordinates (x, y), quadric polynomial transform model is built, and then transform coefficients are worked out by only 6 GCPs or more. We can get initial value of horizontal coordinates of pass points (X_0, Y_0) through transform coefficients.

According to initial value of horizontal coordinates of pass points (X_0, Y_0), we can get initial value of pass point elevation Z_0.

(2)Initial value of ortho-rectification coefficient of each image

Put initial value of ground coordinates of pass points (X_0, Y_0, Z_0) and ground coordinates of GCPs (X, Y, Z) into multi-photo combined adjustment model, initial value of ortho-rectification coefficients of each image (a_{0i}, b_{0i}) is obtained.

2.3.2 Solution of Ground Coordinates of Pass Points and Ortho-rectification Coefficients of Each Image: According to adjustment model, corrected value of ortho-rectification coefficients of each image da_i, db_i and corrected value of ground coordinates of pass points (dX, dY) are gotten. The two kinds of corrected values are computed alternately and iteratively, until (dX, dY) is less than the setting threshold value.

3. EXPERIMENT RESULTS

According to this model, program has been designed. Two experiments have been done on 1m resolution airborne SAR images of study site in Chengdu.

3.1 Experiment Data

Experiment One: Two flight strips, four images, the numbers of strips are 1321, 1309. nine GCPs and ten Pass Points are used. The number of redundant observation is two.

Experiment Two: three flight strips, eleven images, the numbers of strips are 0629, 0707, 0831. nine GCPs and thirty Pass Points are used. The number of redundant observation is six.

Fig.1 is the distribution of images, GCPs(▲) and Pass Points(●) in Experiment One. Fig.2 is the distribution of images, GCPs and Pass Points in Experiment Two.

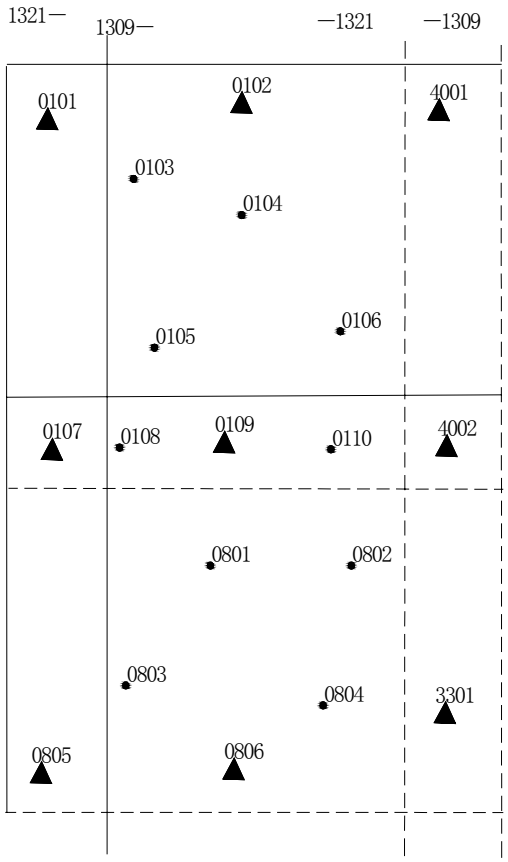

Fig.1 Distribution of GCPs and Pass Points

3.2 Results and Analysis

3.2.1 Experiment One: Table 1 is the combined adjustment accuracy of the four images. The Pass Points are same in Image 1321-01 and 1309-40, Image 1321-08 and 1309-33. So the accuracy of Pass Points is same.

3.2.2 Experiment Two: Table 2 is the combined adjustment accuracy of the eleven images.

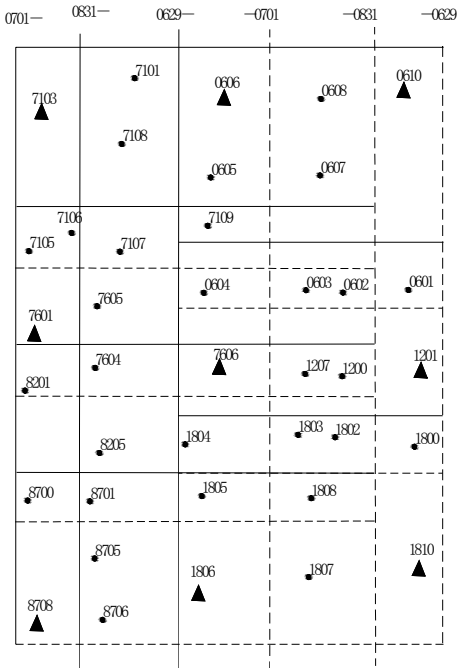

Fig.2 Distribution of GCPs and Pass Points

Image	Mean Square Error(m)			
	X	Y	Z	horizontal
1321-01	2.9	3.4	1.9	4.5
1309-40	2.9	3.4	1.9	4.5
1321-08	2.2	2.4	2.8	3.3
1309-33	2.2	2.4	2.8	3.3
Average	**2.6**	**2.9**	**2.4**	**3.9**

Table 1. Combined Adjustment Accuracy

Image	Mean Square Error(m)			
	X	Y	Z	horizontal
0701-71	1.9	2.1	0.9	2.8
0831-06	1.8	2.5	0.8	3.1
0629-06	0.7	1.3	1.9	1.5
0701-76	1.1	1.6	2.3	1.9
0701-82	1.4	1.6	2.9	2.1
0701-87	1.0	0.8	3.8	1.3
0831-11	1.1	1.2	3.0	1.6
0831-16	1.6	1.2	2.4	2.0
0831-22	1.5	0.7	3.9	1.7
0629-12	1.3	1.4	1.7	1.9
0629-18	1.2	1.3	2.1	1.8
Average	**1.3**	**1.4**	**2.3**	**2.0**

Table 2. Combined Adjustment Accuracy

In the two experiments, the GCPs and the Pass Points are distributed rationally in each image. The two experimental results show that the coordinate accuracy of Pass Points is feasible for 1:10 000 scale ortho-image making and topographic map updating. There are four images in the first experiment, and nine GCPs and ten Pass Points are used. There are eleven images in the second experiment, and nine GCPs and thirty Pass Points are used. The second experimental result is better than the first one. Because the Pass Points are twice overlap in the first experiment and the most Pass Points are more than twice overlap in the second one.

4. CONCLUSIONS

The experimental results show as follows:

Firstly, this method can satisfy accuracy requirement of 1:10，000 scale image ortho-rectification and map updating.

Secondly, compared with conventional ortho-rectification of single image, the number of GCPs has decreased greatly based on this method.

Thirdly, when computing ground coordinates of pass points, the elevation value is obtained from 1:50,000 scale DEM. The experimental results show that the accuracy of pass point is improved enormously used this method.

Fourthly, this method can apply to multi-photo combined adjustment of any airborne SAR image, such as different temporal, different side-looking-orientation, different flight height, different resolution.

According to functions above, this method can also apply in multi-photo spaceborne SAR images and spaceborne SAR images with airborne ones, but time and data is limited, this method will be researched with more kinds of data later.

REFERENCES

Huang G.M., Yue X.J., Zhao Z. et al, 2008. Block Adjustment with Airborne SAR Images Based on Polynomial Ortho-rectification. *Geomatics and Information Science of Wuhan University*, in press.

Zhu C.Y. Xu Q. Wu C.H. et al, 2003. Study on Mathematical Models for Airborne SAR Image Rectification. Journal of Remote Sensing, Vol.7(2), pp. 112-117.

Franz Leberl, 1978. Radar Grammetry For Image Interpretation. *ITC Technical Report*.

G. Domik, Franz Leberl,1988. Radar Image Simulation and Its Application in Image Analysis, *16th ISPRS Congr, Comm. 3*.

Shu N., 2003. Principles of Microwave Remote Sensing[M]. *Chinese Earth quakePress*, pp. 129.

Wang D.H., Liu J., Zhang L., 2005. Precise Rectification of Spaceborne SAR Images Based on Improved F.Leberl Model. *Bulletin of Surveying and Mapping*, Vol(10), pp. 12-15.

Xiao G.C. Zhu C.Y., 2001. Radar Photogrammetry[M]. *Chinese Earth quakePress*, pp. 54-56.

Fan H.D., 2007. Study on Methods of DEM Generation from Airborne Stereo SAR Images[D], *China University of Mining and Technology*.

ACKNOWLEDGEMENT

This work was supported by State Bureau of Surveying and Mapping Key Laboratory of Geographic Information Engineering Foundation of Researches, No 200731.